JOURNAL OF MATERIALS SCIENCE 37 (2002) 4487–4491

The influence of moisture content on the mode I fracture behaviour of sprucewood

A. REITERER
Austrian Industrial Research Promotion Fund (FFF), Kärntner Str. 21-23, A-1015 Vienna, Austria
E-mail: alexander.reiterer@fff.co.at

S. TSCHEGG
Institute of Meteorology and Physics and Christian-Doppler Laboratory for Fundamentals of Wood Machining, Türkenschanzstraße 18, A-1180 Vienna, Austria

The moisture content is known to influence the properties of wood. While mechanical parameters like stiffness and strength decrease with increasing moisture content, investigations on the influence on fracture properties have been concentrated on linear elastic fracture mechanics. In this paper, the wedge splitting method is used to investigate also the non-linear fracture behaviour of sprucewood at different moisture contents. Complete load-displacement curves at four different moisture levels are evaluated. While the initial slope and the maximum stress state are decreasing with increasing moisture content the specific fracture energy is increasing. It is shown that this behaviour can be attributed to an increase in ductility which increases both the dissipated energy during crack initiation and the one in the crack propagation phase.

1. Introduction

Wood, like any other biological material is able to adsorb and desorb water depending on the environmental conditions. It is a well known fact that the wood properties are influenced by the actual reached moisture content (MC), the latter being defined as $\mathrm{MC} = (m_{\mathrm{MC}} - m_{\mathrm{d}})/m_{\mathrm{d}} \cdot 100$, where m_{MC} is the mass at a certain MC and m_{d} the mass in the dried state. Generally, mechanical properties like stiffness or strength decrease with increasing moisture content (see for example [1]). For several parameters studies report maximum values at a MC between 6% and 12% and then a decrease with further drying to very low moisture contents [1, 2]. Above a certain MC, the so called fibre saturation point, the properties stay more or less constant as all bindings for water molecules within the wood structure are saturated. Additional water is incorporated as free water in pores of the macrostructure and microstructure. The fibre saturation point of wood averages in the region around 30% MC, however, in individual species and even in individual pieces of wood it can vary by several percentage points.

In terms of fracture mechanics six principal crack propagation systems exist due to the orthotropic nature of wood. These systems are shown in Fig. 1. When concerning the influence of moisture on the fracture properties much less studies are available in the literature than for mechanical properties. Most of the studies are focused on quantities from linear elastic fracture mechanics like for example stress intensity factors. Analysing the data for the critical energy release rate under Mode I loading from [3, 4] reported that at constant temperature the critical stress intensity factor K_{Ic} increases upon drying below the fibre saturation point but they found a maximum at intermediate MCs for the crack propagation system LT and LR. Petterson and Bodig [5] found that the fracture toughness—MC relationship for a lot of wood species is strongly negative meaning a continuous decrease of fracture toughness with increasing MC in the system TL. However, there have been also reported exceptions for redwood and western redcedar which were attributed to a high extractive content. Sobue and Asano [6] reported lower fracture toughness for a MC of 208% compared to 6.9% in the TR system. Mode I investigations performed by [7] in the TR and TL systems showed a decrease in the K_{Ic} values when the MC was increased from 12% to 18%. Kretschmann and Green [2] investigated both mechanical and fracture mechanical properties of southern pine at different MCs. They reported that both the Mode I and Mode II stress intensity factors increase with decreasing MC from the saturated state to a peak between 7% and 13% MC. However, the peaks were not very pronounced due to the high scatter of the experimental results. Prokopski [8] studied oak and pine at 6%, 9% and 12% MC under loading parallel to the grain. He reported contradicting results, namely a decrease of the K_{Ic} values with increasing MC for pine but an increase for oak. Recently, King *et al.* [9] investigated the Mode I fracture toughness of *Pinus radiata* in all crack propagation systems and found that the Mode I fracture toughness was lower for wet wood in all systems except TR. The Mode II fracture toughness was also lower for wet wood in all systems except LT and LR. In a study

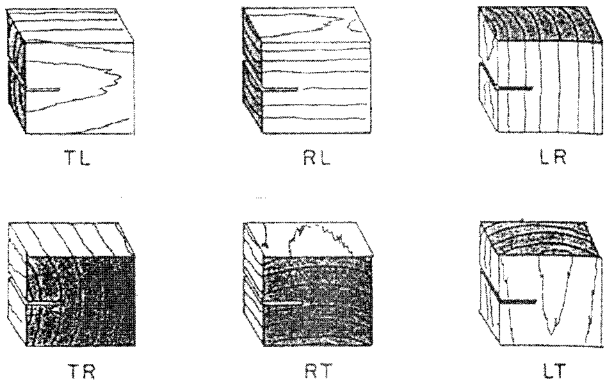

Figure 1 Principal crack propagation systems of wood (see [1]).

TABLE I Examples for values and standard deviations of fracture mechanical parameters as reported in the literature

Author	Fracture system	K_{Ic} (MPam$^{1/2}$)	M.C. (%)	G_f (J/m^2)
Kretschmann and Green [1, 2]	(RT)L	0.51 (0.08)	7	
		0.47 (0.07)	12	
		0.38 (0.08)	18	
		0.29 (0.04)	Saturated	
Schniewind *et al.* [4]	TL	0.23 (0.04)	15	
		0.17 (0.04)	Saturated	
Schniewind *et al.* [7]	TL	0.23 (?)	12	
		0.20 (?)	18	
King et al. [9]	TL	0.28 (0.002)	Dry (?)	
		0.27 (0.03)	Saturated	
	RL	0.49 (0.03)	Dry (?)	
		0.21 (0.1)	Saturated	
Smith and Chui [10]	(RT)L		7	345 (70)
			12	435 (94)
			18	565 (102)
Prokopski [8]	L(RT)	3.47 (0.26)	6	
		2.57 (0.51)	9	
		2.31 (0.45)	12	

performed by [10] the Mode I fracture energy was determined in bending tests. They reported an increase in Mode I fracture energy from the fibre saturation point to 18% MC for crack propagation in the longitudinal direction. Below 18%, any reduction in MC leads to a reduction in fracture energy. As can be seen the results are focused on linear elastic fracture mechanics. A deeper analysis of the reported results shows high variation of the presented data. Examples of the results at different moisture levels and their standard variations are shown in Table I.

Therefore, must of the studies report trends with relatively low statistical significance, especially in the range of 12–18% moisture content. However, a significant conclusion of the reported studies is the fact that the critical stress intensity factor is lower for almost dry wood (moisture contents around 6–7%) compared to saturated wood with moisture contents above 30%.

In this paper Mode I experiments were performed in the RL system using the wedge splitting test at different MCs in order to determine the critical stress intensity factor and also non-linear fracture parameters like the specific fracture energy.

2. Materials and methods

2.1. Materials

Spruce (*Picea abies* [L] Karst) was choosen for this study. Notched specimens as shown in Fig. 2 were prepared in the RL system. The dimensions were the following: $W = 0{,}10$ m; $H = 0{,}13$ m; $T = 0{,}04$ m; $a = 0{,}045$ m; $L = 0{,}085$ m. The starter notch was sharpened using a razor blade. Samples were stored in climate chambers with different temperatures and relative humidities until equilibrium MCs of approximately 12% and 18% were reached. Using a closed box containing salt solutions specimens with an equilibrium MC of 7% could also be conditioned. In order to have samples with a moisture content above the fibre saturation point, beams were stored in water until a MC of approximately 55% was reached. All specimens were stored in the different environments until testing started. At the beginning of the experimental procedure the MC of each sample was determined using an resistance based measurement device. The measured MCs ranges for the four different stored series were (7 ± 0.5)%, (12 ± 0.7)%, (18 ± 1)% and (55 ± 5)%.

Ten samples were investigated for each moisture range. The density of the samples was in the range from 372 kg/m^3 to 442 kg/m^3.

2.2. Experimental procedure

Mode I experiments were performed using the wedge splitting technique as described in detail elsewhere [11–14]. The basic idea is that a notched specimen resting on a linear support is splitt by help of a load transmission equipment which is situated in a groove of the specimen. The principle can be seen in Fig. 3. The horizontal splitting force F_H is calculated from the force of the testing machine F_M according to

$$F_H = F_M/2\tan(\alpha/2), \tag{1}$$

where α denotes the wedge angle. As the force from the machine is transmitted by roll bodies friction can be neglected. The displacement δ was determined using an optical measurement system as described in [15]. From the whole load displacement curve the specific fracture energy G_f was determined according to

$$G_f = \frac{1}{A}\int_0^{\delta\,\max} F_H(\delta)\,d\delta \tag{2}$$

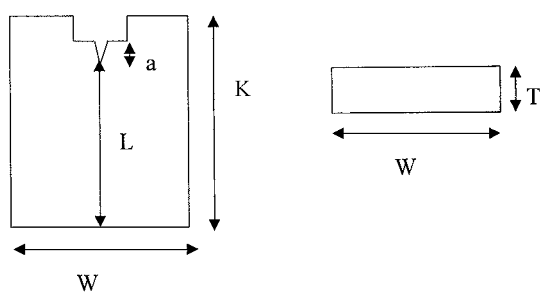

Figure 2 Specimen geometry of the splitting samples.

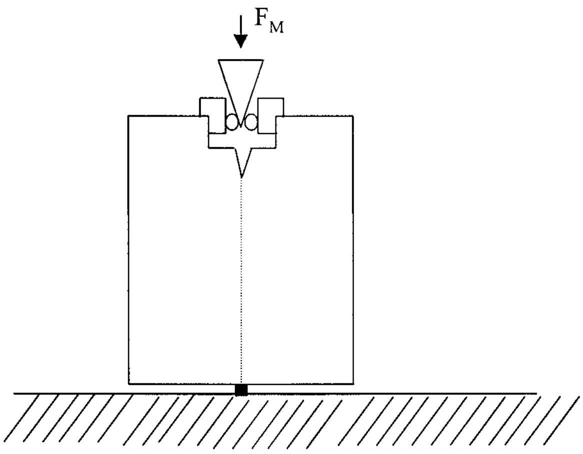

Figure 3 Principle of the Mode I wedge splitting test [11].

where A is the fracture surface. This quantity is a "toughness" quantity characterizing the entire Mode I fracture process until the specimen is split into two halves and does not depend on specimen size and shape if the specimen size is not too small. The used size is large enough to obtain size independent values for spruce [12].

In order to characterize also the stress state when crack propagation occurs the maximum horizontal splitting force $F_{\mathrm{H,max}}$ was used to determine the critical stress intensity factor K_{Ic}. The specimen geometry was chosen such that a known geometry factor could be used [16]. The critical stress intensity factor was evaluated according to

$$\begin{aligned} K_{\mathrm{Ic}} &= \left(F_{\mathrm{H.max}}/BH^{1/2}\right)(1-a/H)^{-3/2} \\ &= F_{\mathrm{H.max}} Y(a, H, B) \end{aligned} \qquad (3)$$

where H is the distance between the acting line of the horizontal force and the bottom of the specimen and a is the notch length. With the geometry used the factor Y is equal to $Y = 389.1\ \mathrm{m}^{-3/2}$. This evaluation does not consider the orthotropic nature of wood but as shown previously in the RL crack propagation system such an isotropic approximation is justified [17].

The initial slope k_{init} of the load displacement curves has also been determined to characterize the stiffness of the samples and is proportional to an effective modulus of elasticity [18]. As specimen geometry and size was the same for all wood species and orientations the initial slopes can be compared.

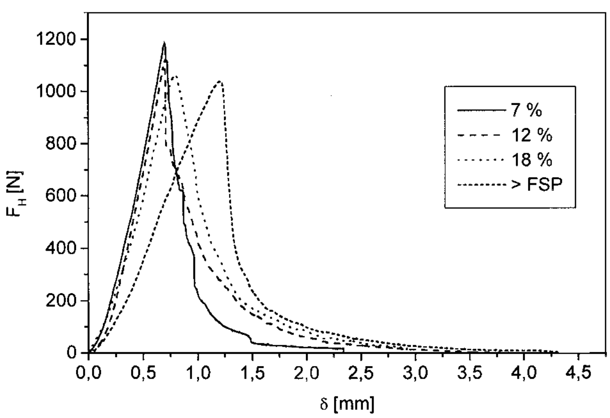

Figure 4 Represantative load-displacement curves at different moisture content.

3. Results and discussion

In Fig. 4 typical load-displacement curves for the different moisture contents are shown. As can be seen the fracture behaviour is clearly influenced by moisture

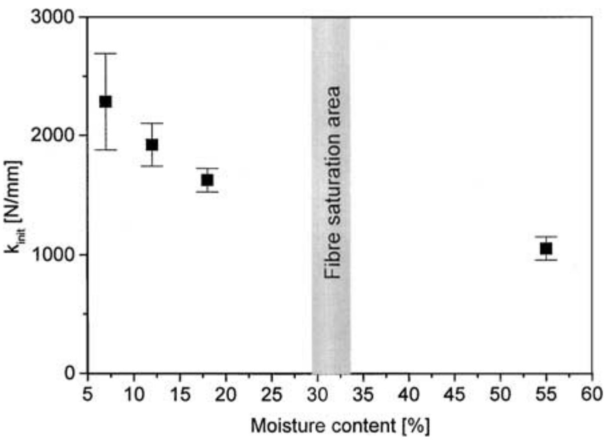

Figure 5 Initial slope K_{init} as a function of moisture content. The error bars indicate the standard deviation.

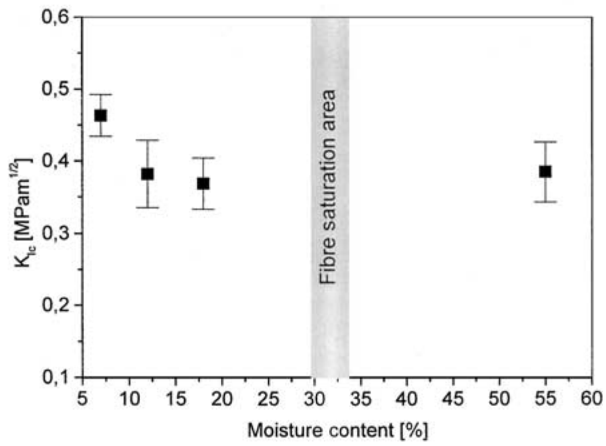

Figure 6 Critical stress intensity factor K_{Ic} as a function of moisture content. The error bars indicate the standard deviation.

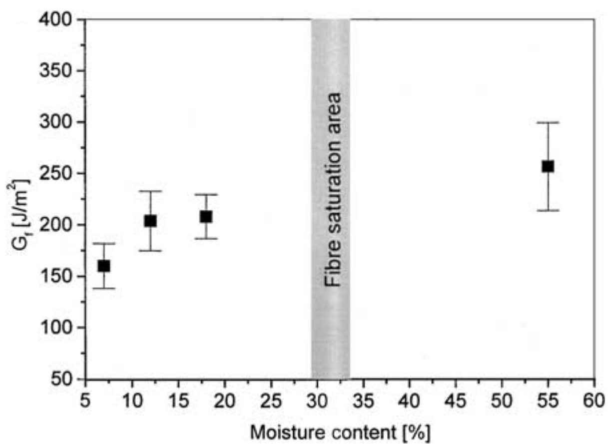

Figure 7 Specific fracture G_{f} as a function of moisture content. The error bars indicate the standard deviation.

content. The curves indicate already a decrease in the maximum stress state and an increase in the displacements with increasing moisture content.

The initial slope k_{init} is shown in Fig. 5. A trend of decrease with increasing moisture content is visible. A one-way ANOVA (analysis of variance for a quantitative dependent variable by a single factor variable) shows that only the values at 7% and 12% MC are not significantly different ($P < 0.05$). As the initial slope is proportional to an effective modulus of elasticity under the loading conditions with a force acting perpendicular to the grain the results are in good agreement with the literature about conventional mechanical investigations on the modulus of elasticity perpendicular to the grain [2]. This holds also for the amount of reduction, the fibre saturated samples with a initial slope around 1000 N/mm reach only 43% of the ones at 7% MC which show values around 2300 N/mm.

The critical stress intensity factor K_{Ic} is shown in Fig. 6. The general trend is similar as a decrease from a moisture content of 7% to a moisture content of 55% is visible. However, the reduction is significant from a MC of 7% to a MC of 12% as the analysis shows that the value at 7% MC is significantly different from all other values ($P < 0.05$). For higher MC's the fracture toughness stays more or less constant. Compared to the values at 7% MC (0.47 MPam$^{1/2}$) saturated wood reaches approximately 75% of this values (0.37 MPam$^{1/2}$). Therefore, the reduction is not as high as for the initial slope. A maximum at intermediate MCs as reported in [4],

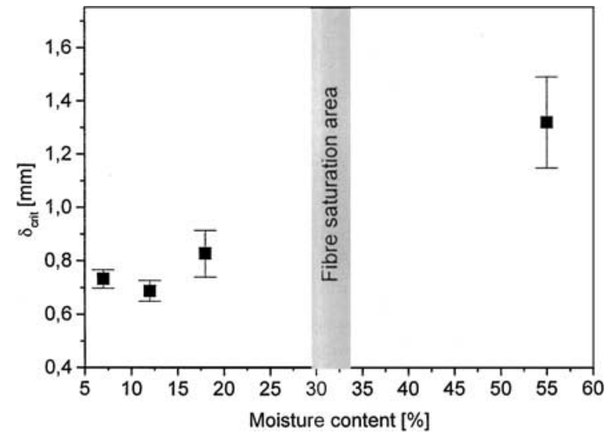

Figure 8 Critical displacement at crack initiation as a function of moisture content. The error bars indicate the standard deviation.

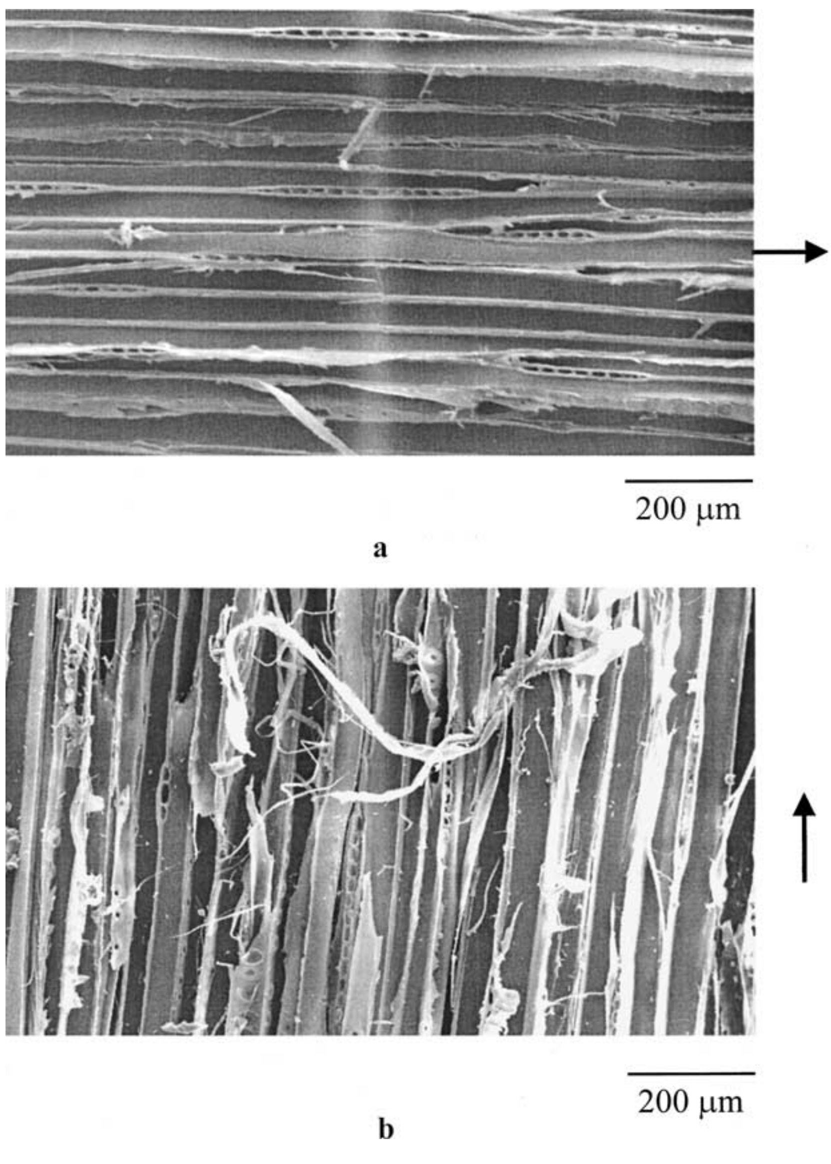

Figure 9 Typical fracture surface of at 7% moisture content (a) and at 55% moisture content (b). The arrows indicate the macroscopic fibre direction.

could not be found. The slight reduction with increasing MC is much more in agreement with the results reported by [2, 8]. Having in mind that the variations of the reported data in the literature is high as mentioned in the introduction the statement of higher values of the critical stress intensity factor for almost dry wood compared to saturated wood is in agreement with previous results.

The results for the specific fracture energy G_f show a different situation. As depicted in Fig. 7 the specific fracture energy is increasing with increasing moisture content. This means that more energy per unit area is needed for higher MCs to separate a wood sample into two halves. The performed one-way ANOVA shows that the value at 7% MC is significantly different from all other values ($P < 0.05$). The one at saturated state is different to the one at 12% MC ($P < 0.05$) and at a lower level also to the one at 18% MC ($P < 0.1$). Therefore, the above mentioned statement seems justified.

The whole fracture process can be roughly subdivided into two parts. First, there is the energy dissipated in the crack initiation phase. This energy is needed to form the process zone around the crack tip (microcrack, irreversible deformations, etc.). The energy which has been applied to propagate the crack is the sum of the area under the load displacement curve from the maximum load to complete separation of the specimen and the elastic stored energy which is dissipated during crack propagation. The energy needed to form the process zone before the macrocrack starts to propagate is increasing which can be explained by the fact that the ductility and therefore the dissipation of energy due to irreversible deformations is increased by an increased MC. This interpretation may be supported by the fact that the critical crack opening displacement as shown in Fig. 8 is larger for MCs above the saturation area which means that the material can be strained more until crack propagation starts. The value at saturated state is significantly different from all others ($P < 0.05$).

On the other hand processes like fibre bridging behind the crack tip should also consume more energy when the material becomes more ductile and the contribution of the crack propagation phase to the fracture energy can also be expected to increase. Therefore, the conclusion seems justified that the reason for an increase in specific fracture energy with increasing MC, especially compared to the saturated state, is an increase in ductility. The higher ductility overcompensates the reduction of the stiffness and the maximum stress state leading in sum to an increased specific fracture energy.

Scanning electron microscope images support the above interpretation. In Fig. 9a the typical fracture surface of a sample with 7% MC is depicted. In Fig. 9b the fracture surface of a specimen with 55% MC is shown. It can be seen well, that the fracture surface of the wet sample is deformed more. A lot of long cell wall fragments torn out of the cell walls are visible. The tracheids are deformed more and one can imagine that the long cell wall fragments can act as fibre bridges in the crack propagation phase.

4. Conclusions

The influence of moisture content on the Mode I fracture behaviour of sprucewood has been investigated using the wedge spitting method. It could be shown that a higher moisture content increases the ductility whereas the stiffness characterized by the initial slope of the obtained load-displacement curves and also the maximum stress state characterized by the critical stress intensity factor decreases. The increase in ductility leads to a significant increase of the specific fracture energy characterizing the entire fracture process.

Acknowledgement

The authors thank the University of Agricultural Sciences for having financed the ESEM and they acknowledge financial support of these studies by Hilti AG, Principality of Liechtenstein, within the CD-Laboratory.

References

1. "Wood Handbook—Wood as an Engineering Material" (Forest Products Society, USA, 1999) p. 4.
2. D. E. KRETSCHMANN and D. W. GREEN, *Wood Fiber Sci.* **28** (1996) 320.
3. A. W. PORTER, *Forest Prod. J.* **14** (1964) 325.
4. A. P. SCHNIEWIND, T. OHGAMA, T. AOKI and T. YAMADA, *Wood Science* **15** (1982) 101.
5. R. W. PETTERSON and J. BODIG, *Wood Fiber Sci.* **15** (1983) 302.
6. N. SOBUE and A. ASANO, *Mokuzai Gakkaishi* **33** (1987) 7.
7. A. P. SCHNIEWIND, S. L. QUARLES and S.-H. LEE, *Wood Sci. Technol.* **30** (1996) 273.
8. G. PROKOPSKI, *Int. J. Fract.* **79** (1996) R73.
9. M. J. KING, I. J. SUTHERLAND and L. LE-NGOC, *Holz Roh-Werkstoff* **57** (1999) 235.
10. I. SMITH and Y. H. CHUI, *Wood Sci. Technol.* **28** (1994) 147.
11. E. K. TSCHEGG, Patent AT-390328, 1986.
12. S. E. STANZL-TSCHEGG, D. M. TAN and E. K. TSCHEGG, *Wood Sci. Technol.* **29** (1995) 31.
13. R. J. A. EHART, S. E. STANZL-TSCHEGG and E. K. TSCHEGG, *ibid.* **32** (1998) 43.
14. A. REITERER, S. E. STANZL-TSCHEGG and E. K. TSCHEGG, *ibid.* **34** (2000) 417.
15. G. SINN, A. REITERER, S. E. STANZL-TSCHEGG and E. K. TSCHEGG, *Holz Roh-Werkstoff* **59** (2001) 177.
16. G. ZHAO, H. JIAO and S. XU, in Proc. of RILEM/ESIS Conference Fracture Processes in Concrete, Rock and Ceramics, Noordwijk, The Netherlands, edited by J. G. M. van Mier, J. G. Rots and A. Baker (E&FN Spon, 1991).
17. H. SCHACHNER, A. REITERER and S. E. STANZL-TSCHEGG, *J. Mater. Sci. Lett.* **19** (2000) 1783.
18. H. HARMUTH, K. RIEDER, M. KROBATH and E. K. TSCHEGG, *Mat. Sci. Eng.* A **214** (1996) 53.

Received 18 April 2001
and accepted 3 June 2002